CONF-881115--1

<The Third International Topical Meeting on Nuclear Power Plant Thermal Hydraulics and Operations, Nov. 14-17, 1988, Seoul, Korea>

Thermally Induced Flow Oscillation in Vertical Two-phase Natural Circulation Loop

CONF-881115--1

DE88 010066

Sang Yong Lee
Department of Mechanical Engineering
Korea Advanced Institute of Science and Technology
P.O. Box 150, Cheong Ryang, Seoul, Korea

and

Mamoru Ishii
Reactor Analysis and Safety Division
Argonne National Laboratory
9700 S. Cass Avenue
Argonne, Illinois 60439, U.S.A.

Abstract

In order to study the two-phase natural circulation during a small break loss of coolant accident in LWR, simulation experiments have been performed using Freon-113 boiling and condensation loop. In quasi-steady state, the flow became relatively stabilized and certain regular patterns of flow oscillations were detected with ranges of periods in 8~35 seconds and 2.5~4 minutes. In order to find out the nature of these oscillations, one-dimensional field equations for the single-phase (liquid) and two-phase region were set up, and these field equations were integrated along the loop. The homogeneous flow model was used for the two-phase region. Then the characteristic equation was derived using perturbation method. Thermal non-equilibrium and compressibility of each phase were not considered in the present analysis. The characteristic equation derived can be used to obtain the stability criteria. A simplified approach showed that the short-period oscillation were the manometer oscillation. The longer period oscillations were the density wave oscillation which had the period of oscillations close to the residence time of a fluid around the loop.

Nomenclature

a	Constant (length)
A	Cross-sectional area
b	Constant (length)
c	Constant (length)
C_I, C_{II}, C_{III}	Constants
d	Constant (length)
D	Diameter
f	Friction factor
g	Gravity
H	Characteristic function
i	Enthalpy
K	Friction resistance coefficient of the valve
ℓ_o	Constant (length)
L	Constant (length)
P	Pressure
ΔP	Pressure difference
δP	Perturbed pressure
q	Heat flux
Q	Volumetric flow rate
$\dot{Q}$	Heat flow rate
S	Complex variable
t	Time
u	Velocity
δu	Perturbed velocity
v	Specific volume
x	Quality

z	Axial coordinate

Greek Symbols

α	Void fraction
ε	Amplitude of perturbed velocity
ξ	Heated (wetted) perimeter
Λ	Boiling/condensing boundary
ρ	Density
σ	Growth rate of amplitude
τ	Residence time
ω	Angular frequency of oscillation
ζ	Damping ratio
Ω	Reaction frequency

Subscripts

c	Cooling
f	Saturated liquid
fg	Quantity between saturated vapor and liquid
g	Saturated vapor
h	Heating
k	Friction control valve
ℓ	Liquid region
t	Two-phase region
1,...,6	Flow boundaries

Superscripts

-	Time-averaged value

I. Introduction

In order to study the two-phase natural circulation and flow termination during a small break loss of coolant accident in LWR, simulation experiments have been performed using two different thermal-hydraulic loops [1]. The main focus of the experiment was placed on the two-phase flow behavior in the hot-leg U-bend typical of B&W LWR systems. The first group of experiments was carried out in the nitrogen gas-water adiabatic simulation loop and the second in the Freon-113 boiling and condensation loop. Both of the loops have been designed and built according to the two-phase flow scaling criteria developed previously [2-6]. The nitrogen gas-water system has been used to isolate key hydrodynamic phenomena such as the phase distribution, relative velocity between phases, two-phase flow regimes and flow termination mechanisms, whereas the Freon loop has been used to study the effect of fluid properties, phase changes and coupling between hydrodynamic and heat transfer phenomena. In the Freon-113 loop, phase change phenomena created much more unstable hydrodynamic conditions which lead to cyclic or oscillatory flow behaviors. In view of this, the nature of the flow oscillations in vertical two-phase natural circulation loop were studied in detail.

II. Experimental Observations

1. Description of the Experimental Loop

The schematic of the primary loop is shown in Fig. 1. This Freon-113 boiling and condensation loop was designed such that it could be operated either in a natural or in a forced circulation mode. The primary loop consists of the heater section (or simulated core), hot-leg, U-bend, condenser simulating a steam generator, subcooler, friction control valve, expansion tank and pump. The loop pressure is regulated by the pressure at the free surface in the expansion tank. This pressure is maintained close to the atmospheric pressure by two pressure relief valves for the positive and negative pressure cracking. Due to the hydrostatic head of the liquid Freon-113, the pressure at the simulated core is always above the atmospheric pressure, up to 159 KPa (23 psia). Basically, the two phase flow is generated by boiling of Freon-113 in the simulated core and condensed in the simulated steam generator which is cooled by the secondary loop. Freon-113 has a low saturation temperature of about 47°C at 1 atm. Thus the loop is operated at relatively low pressures and temperatures. The components and sections involving two-phase flow are designed to be transparent such that a flow visualization is possible. At present, the loop is approximately 6 m in height with the hot-leg inner diameter of 5 cm and the vertical elevation of about 5 m. The transparent sections were made of standard Corning Pyrex glass pipes and fittings. Other sections were made of copper tubes, brass fittings and stainless steel components.

The secondary loop which is connected to S1 in Fig. 1 is used to cool the condenser of the primary loop. The secondary loop consists of the circulation pump, condenser coil inside the simulated steam generator, heat exchanger cooled by tap water, and coils submerged in a cold bath within a large chest-type freezer. Freon-113 is also used as a coolant in the secondary loop. The secondary loop is pressurized to 0.28 MPa above the atmospheric pressure (40 psig) and the coolant is always in the liquid state. Therefore, the thermal hydraulics of the secondary loop is not simulated in the present facility.

The heater section has seven immersion heaters with total power of 4.2 KW, controlled by two variac transformers. This total power was determined based on the scaling law corresponding to decaying heat of 2% of full power in the prototype system with two hot-legs.

The two loops have several temperature measurements in addition to the hydrodynamic instrumentations such as the differential pressure transducers, pressure gauges and flowmeters. The pressure lines have special bubble purging devices to eliminate gas or vapor bubbles from the pressure transducers and pressure lines. All the analog signals from the thermocouples, pressure transducers, and flowmeters (turbine type) are read through the DASH-8 A/D board with two EXP-16 multiplexer boards and a STA-08 screw termination accessory board into the IBM-PC/XT using LTN (Labtech Notebook) software.

2. Flow Behavior

Experimental measurements were performed using the Freon-113 loop with experimental conditions shown in Table I.

Table I. Experimental Conditions

Experimental Parameters	Conditions
Friction Control Valve Opening	Full, 1/4
Power (Heat) Input	1.3 KW, 2.2 KW
Secondary Loop Cooling	High, Medium, Low and No Cooling

The two-phase natural circulation flow was initiated by the unsteady, cyclic behavior of two-phase flow involving sudden flashing and subsequent suppression of boiling with temporal flow termination. This unsteady behavior is described in detail elsewhere [1,7]. As the unsteady behavior continues, the whole flow phenomena reach a certain quasi-steady state with relatively stabilized flow. At this stage certain regular patterns of flow oscillations were detected. Figures 2 and 3 show two different types of oscillations which are named as Type 1 and Type 2, respectively. Along with those two different types of oscillations, two dominant ranges of periods of oscillations were detected; they are 8~35 sec. and 2.5~4 min., respectively. For example, in Fig. 2(c)-(h), Type 1 oscillation with oscillatory period of ~20 sec. is clearly observed. Or, as in Fig. 3(a) and Fig. 3(c)-(h), Type 2 oscillation with two dominant frequencies (~35 sec. and ~3 min.) is observed. At the beginning of each cycle of Type 1 oscillation, the liquid level in the heater section is slightly higher than the horizontal outlet of the heater section connected to the riser section of the hot-leg. Due to the regular oscillation of the liquid level with continuous boiling inside the heater section, the liquid level gradually approaches the horizontal outlet and the vapor begins to flow into the riser section. The temperature inside the riser section remains almost in the saturated condition corresponds to the hydrostatic pressure. Since the hydrostatic pressure decreases along the riser section, the fluid flowed into the bottom of the hot-leg becomes slightly superheated as it climbs up. Thus the vapor introduced into the riser section becomes a short slug bubble by evaporation and flashing (see the sharp peaks of the void fractions in Fig. 2(e)-(h)) as it moves up, which induces a sizable amount of flow carry-over through the inverted U-bend (see the peaks of the flow rate in Fig. 2(d)). This disturbs and changes the liquid levels inside the simulated steam generator and the heater section temporarily, and the whole process repeats with a cyclic period of ~20 sec. Unlike the initial stage, the temperature inside the heater section remains at the saturated condition. This is due to the lower subcooling and smaller amount of incoming liquid into the heater section compared to the unsteady case, and does not change the temperature of fluid inside the heater section.

In Type 2 oscillation, the liquid level in the heater section remains almost stationary with continuous flow of vapor into the riser section. The flow carry-over is maintained by bubbly flow generated by continuous evaporation and slow boiling; thus the void fraction becomes very steady with a longer period (2.5~4 min.) of oscillations (see Fig. 3(e)-(f)). Also, the liquid level inside the simulated steam generator, which can be regarded as the condensation front, oscillates with the same cyclic period. Along with this longer period the oscillations with ~35 second-period are also observed (Fig. 3(d)), though the period is not very regular.

The types of oscillations depend strongly on the liquid level inside the simulated steam generator as well as the experimental boundary conditions imposed. This is explained in detail elsewhere [7].

In order to find out the nature of those oscillations, a preliminary analysis was carried out in the following section.

III. Preliminary Analytical Considerations

Freon-113 boiling and condensation loop is simplified as a one-dimensional vertical two-phase natural circulation loop as shown in Fig. 4. It is assumed that the heat is applied at the heater section with uniform heat flux q_h and removed at the condenser section with uniform heat flux q_c. From the overall energy balance of the loop, the incoming heat, $q_h(d-c)$, should be same as the outgoing heat, $q_c(a-b)$. The pressure inside the loop is assumed to be almost uniform and constant, and the non-equilibrium effect is not considered. Thus the physical properties of the fluid are assumed to be constant and the mixture density in the two-phase region depends only on the enthalpy. As a simple two-phase flow approach, homogeneous flow was assumed.

1. Governing Field Equations

As shown in Fig. 4, the loop was divided into six flow regions with their boundaries denoted as 1 '... 6 '; they are unheated liquid region (⑥'~①'), heated liquid region (①'~②'), heated two-phase region (②'~③'), unheated two-phase region (③'~④'), cooled two-phase region (④'~⑤') and cooled liquid region (⑤'~⑥') respectively. Also, the points ②' and ⑤' imply boiling and condensation boundaries respectively. The loop has a long horizontal section of length ℓ_0 and a loop friction control valve in the unheated liquid region.

The governing equations for each region can be expressed as follows:

Continuity Equation

$$\frac{\partial \rho}{\partial t} + u \frac{\partial \rho}{\partial z} + \rho \frac{\partial u}{\partial z} = 0 \ . \tag{1}$$

Momentum Equation

$$- \frac{\partial P}{\partial z} = \rho \frac{\partial u}{\partial t} + \rho u \frac{\partial u}{\partial z} + \rho g + \frac{f}{2D} \rho u^2 \ . \tag{2}$$

Energy Equation

$$\frac{\partial i}{\partial t} + u \frac{\partial i}{\partial z} = \frac{q\xi}{\rho A} \ . \tag{3}$$

Here, ρ, u, i, q and f stand for density, velocity, enthalpy, heat flux and friction factor in each region.

The value of q in the energy equation (Eq. (3)) is zero in unheated regions (⑥'~①' and ③'~④'), $-q_c$ in cooled regions (④'~⑤' and

⑤'~⑥') and q_h in heated regions (①'~②' and ②'~③'). In addition to above equations, the equation of state,

$$v_t = v_f + \frac{\Delta v_{fg}}{\Delta i_{fg}} (i_t - i_f) \tag{4}$$

is needed for the heated and cooled two-phase regions (②'~③' and ④'~⑤') to count for the density changes due to boiling and condensation. Here v denotes the specific volume. For the unheated liquid region (⑥'~①'), the pressure drop across the friction control valve can be expressed as

$$\Delta p_k = \frac{1}{2} K \rho_\ell u_\ell^2 , \tag{5}$$

where K stands for the friction resistance coefficient of the valve.

2. Method of Approach

For a stability analysis of a flow system the perturbation technique with linearization is one of the most effective approaches. In the present analysis, the disturbance will be given in terms of the fluctuation of the liquid velocity. The inlet liquid velocity at the heater section, u_ℓ, is divided into the steady state term, $\bar{u}_\ell$, and the perturbed velocity term, δu_ℓ, thus

$$u_\ell = \bar{u}_\ell + \delta u_\ell \; . \tag{6}$$

For the frequency-response method the perturbation velocity δu_ℓ is given by an exponential function as

$$\delta u_\ell = \varepsilon\, e^{St} , \tag{7}$$

$$\text{where } S = \sigma + j\omega \tag{8}$$

$$j = \sqrt{-1} . \tag{9}$$

Here S is a complex number, and the real part gives the amplitude coefficient whereas the imaginary part represents the angular frequency of oscillation. For the linear-perturbation analysis, ε is assumed to be very small compared to the average liquid velocity $\bar{u}_\ell$, and only the first order terms in the perturbed equations are retained for the analysis. First, the continuity and energy equations are solved by decoupling them from the momentum equation. Then the momentum equations for each region were integrated along the loop. From these solutions the characteristic equation which is a function of time only is derived using the perturbation method with the linearization assumption. The detailed derivations are quite lengthy and were not presented in this paper. However, the resulting characteristic equation can be expressed in the following form:

$$H(S) = H\left(S, \frac{1}{S}, \frac{1}{S-\Omega_h}, \frac{1}{S-2\Omega_h}, \frac{1}{S+\Omega_c}, \frac{1}{S+2\Omega_c}, \right.$$

$$\left. e^{-S\bar{\tau}_{12}}, e^{-S\bar{\tau}_{23}}, e^{-S\bar{\tau}_{34}}, e^{-S\bar{\tau}_{45}}, e^{-S\bar{\tau}_{56}}, e^{-S\bar{\tau}_{61}}\right) = 0 , \tag{10}$$

where, Ω_h and Ω_c denote the reaction frequencies for heating and cooling defined by

$$\Omega_h \equiv -\frac{1}{\rho^2}\frac{d\rho}{di}\frac{q_h \xi}{A} \tag{11}$$

$$\Omega_c \equiv -\frac{1}{\rho^2}\frac{d\rho}{di}\frac{q_c\xi}{A} \tag{12}$$

with q_h and q_c being the absolute positive values.

The characteristic times given by $\bar{\tau}_{12},\ldots,\bar{\tau}_{61}$ are the time averaged residence times in Lagrangian description at each section of the loop, and defined by

$$\bar{\tau}_{12} = \frac{\rho_\ell A}{q_h\xi}\left(i_f - \bar{i}\right) \tag{13}$$

$$\bar{\tau}_{23} = \ell n\left[\frac{\Omega_h\left(d-\bar{\Lambda}_2\right) + \bar{u}_\ell}{\bar{u}_\ell}\right]^{1/\Omega_h} = \ell n\left[\frac{\bar{u}_t}{\bar{u}_\ell}\right]^{1/\Omega_h} \tag{14}$$

$$\bar{\tau}_{34} = \frac{2L - a - d}{\Omega_h\left(d-\bar{\Lambda}_2\right) + \bar{u}_\ell} = \frac{2L - a - d}{\bar{u}_t} \tag{15}$$

$$\bar{\tau}_{45} = \frac{\Omega_h}{\Omega_c}\bar{\tau}_{23} \tag{16}$$

$$\bar{\tau}_{56} = \frac{\Omega_h}{\Omega_c}\bar{\tau}_{12} \tag{17}$$

$$\bar{\tau}_{61} = \frac{b + \ell_o + c}{\bar{u}_\ell}, \tag{18}$$

where

$$\bar{\Lambda}_2 = \bar{u}_\ell\bar{\tau}_{12} + c, \tag{19}$$

which is the boiling boundary at the heater section. Thus, the total residence time of the fluid around the loop will be

$$\bar{\tau} = \bar{\tau}_{12} + \bar{\tau}_{23} + \bar{\tau}_{34} + \bar{\tau}_{45} + \bar{\tau}_{56} + \bar{\tau}_{61} \; . \tag{20}$$

Hence, the relationship between the perturbation of the pressure drop along the loop and the perturbation of the incoming velocity of liquid to the heater section can be described as

$$\delta\Delta P = H(S)\delta u_{\ell} \; . \tag{21}$$

In other words, the input force imposed on the system is $\delta\Delta P$ and it induces the change of flow by δu_{ℓ}. Thus, the dynamic response can be represented by the transformation

$$\delta u_{\ell} = \frac{1}{H(S)} \delta\Delta P \; , \tag{22}$$

where $1/H(S)$ represents the system transfer function. According to the stability theory, the asymptotic stability of the system can be determined from the nature of the roots of the characteristic equation

$$H(S) = 0 \; . \tag{23}$$

The detailed stability analysis of this system is beyond the scope of this paper and will be shown elsewhere.

3. Simplified Approach

As can be seen from the form of Eq. (10), it is not possible to solve the original characteristic equation analytically, thus it is necessary to solve it numerically. However, for a simpler case, an analytical approach may be possible. In what follows, some simple cases are discussed in detail. Let the heater section and simulated steam generator be the point heat source and sink respectively. That is, in Fig. 4, the region ①'~③' turns into a single point heat source and also the region ④'~⑥' turns into a single point heat sink. They are denoted as points ②' and ⑤' respectively, and those two points (i.e., phase-changing boundaries) are assumed to be not fixed in space. In the two-phase region ρ_t and u_t are assumed to be uniform. Then from Eq. (1),

$$\frac{\partial \rho_\ell}{\partial t}, \frac{\partial \rho_t}{\partial t} = 0 \tag{24}$$

which implies

$$\rho_\ell, \rho_t = \text{const} \tag{25}$$

and

$$x = \text{const} . \tag{26}$$

Thus, under the assumption the density wave propagation velocity is infinite in each region. Thus, with same constant heat flow rate for boiling and condensation (i.e., $\dot{Q}_h = \dot{Q}_c$), it can be shown that

$$\frac{d\Lambda_2}{dt} = - \frac{d\Lambda_5}{dt} , \tag{27}$$

Then each region acts as a lumped mass. This also implies that the length of the liquid column remains constant.

From Eq. (2), the momentum equations can be rewritten for the single-phase and two-phase region as follows:

$$\frac{\partial}{\partial t} (\rho_\ell u_\ell) = - \frac{\partial P}{\partial z} - \rho_\ell g - \frac{f_\ell}{2D} \rho_\ell u_\ell^2 \tag{28}$$

$$\frac{\partial}{\partial t} (\rho_t u_t) = - \frac{\partial P}{\partial z} - \rho_t g - \frac{f_t}{2D} \rho_t u_t^2 . \tag{29}$$

Also, from the continuity between the two regions it is necessary that

$$\rho_t u_t = \rho_\ell u_\ell - (\rho_\ell - \rho_t) \frac{d\Lambda_2}{dt} . \tag{30}$$

From the energy balance around the point heat source,

$$\rho_\ell A \left(u_\ell - \frac{d\Lambda_2}{dt} \right) \Delta i_{fg} x = \dot{Q}_h , \tag{31}$$

This can be rewritten as

$$u_\ell = \frac{\dot{Q}_h}{\rho_\ell A \Delta i_{fg} x} + \frac{d\Lambda_2}{dt} . \tag{32}$$

Since x and $\dot{Q}_h$ are constant, the first term of the right-hand side of Eq. (32) is the time-averaged value and the second term is the fluctuating component. Thus

$$\delta u_\ell = \frac{d\Lambda_2}{dt} \, . \tag{33}$$

Next Eqs. (28) and (29) are integrated and the solutions are combined by using Eqs. (6), (30) and (33) with the pressure drop across the friction control valve (Eq. (5)) taken into account. Then, by differentiating it with respect to time using Eqs. (6), (27) and (33) with the higher order terms of the fluctuation neglected, the following result can be obtained

$$C_I \frac{d^2}{dt^2} (\delta u_\ell) + C_{II} \, \rho_\ell \bar{u}_\ell \frac{d}{dt} (\delta u_\ell) + 2C_{III} (\delta u_\ell) = 0 \, , \tag{34}$$

where

$$C_I = (2L - \bar{\Lambda}_2 - \bar{\Lambda}_5)\rho_t + (\ell_o + \bar{\Lambda}_2 + \bar{\Lambda}_5)\rho_\ell \tag{35}$$

$$C_{II} = \frac{f_t}{D} (2L - \bar{\Lambda}_2 - \bar{\Lambda}_5) + \frac{f_\ell}{D} (\ell_o + \bar{\Lambda}_2 + \bar{\Lambda}_5) + K \tag{36}$$

$$C_{III} = (\rho_\ell - \rho_t)g \, . \tag{37}$$

Or with Eq. (7), Eq. (34) can be expressed as

$$C_I \, S^2 + C_{II} \cdot \rho_\ell \bar{u}_\ell \, S + 2C_{III} = 0 \, . \tag{38}$$

This equation has the form of the one-degree-of-freedom oscillation, and C_I, C_{II}, C_{III} stand for the mass of the fluid, loop friction and restoring force by gravity respectively. Thus, it can be concluded that the above analysis gives the manometer type oscillation. The procedure to solve this second order equation is straightforward. The angular frequency of oscillation is obtained as

$$\omega_d = \omega_n \sqrt{1 - \zeta^2} \ , \tag{39}$$

where

$$\omega_n = \sqrt{\frac{2C_{III}}{C_I}} \ , \tag{40}$$

and

$$\zeta = \frac{\rho_\ell \bar{u}_\ell C_{II}}{\sqrt{8C_I C_{III}}} \ . \tag{41}$$

For a sample calculation of the case corresponding to Fig. 2, various conditions are given in Table II. The friction resistance coefficient for the entire loop measured experimentally with the position of the friction control valve at fully open was about 37 [7]. This value is used for the value of C_{II}. The calculated result showed that the angular velocity, ω_d, was 0.651 rad/sec, and the period of oscillation was 9.6 sec. Since the loop shown in Fig. 1 has several different cross-sectional areas, the actual value of the period of oscillation is considered to be somewhat longer. From Fig. 2, it can be seen that the period of the corresponding oscillations have the period of ~20 sec. Thus from the simplified analysis it should be the manometer oscillation. For the case of Fig. 3, the value of K is very large due to small opening of the friction control valve and so does the C_{II} value in Eq. (36). Thus from Eq. (41), the value for ζ becomes large and the period of oscillation should increase close to ~35 sec. Therefore, the flow oscillations detected with the range of period in 8~35 seconds were manometer oscillations. It is noted that Eq. (38) can also be obtained directly from the original characteristic equation by making the following assumptions similar to those for the simplified analysis.

$$c = d = \bar{\Lambda}_2$$

$$a = b = \bar{\Lambda}_5 \tag{42}$$

$$\bar{\tau}_{12}, \bar{\tau}_{23}, \bar{\tau}_{45}, \bar{\tau}_{56} << \bar{\tau}_{61}, \bar{\tau}_{34},$$

Under these conditions the characteristic becomes

$$H(S) = \Bigg[S(\bar{\tau}_{34} + \bar{\tau}_{61}) + \left\{ K + \frac{f_\ell}{D} (\bar{\Lambda}_2 + \bar{\Lambda}_5 + \ell_o) + \frac{f_t}{D} (2L - \bar{\Lambda}_2 - \bar{\Lambda}_5) \right\}$$

$$+ \frac{1}{S-\Omega_h} \left\{ S \left(-\ell n \left(\frac{\bar{u}_\ell}{\bar{u}_t} \right) \right) + \frac{g}{\bar{u}_\ell} \left(1 - \frac{\bar{u}_\ell}{\bar{u}_t} \right) \right\}$$

$$+ \frac{1}{S+\Omega_c} \left\{ S \left(\ell n \left(\frac{\bar{u}_\ell}{\bar{u}_t} \right) \right) + \frac{g}{\bar{u}_\ell} \left(1 - \frac{\bar{u}_\ell}{\bar{u}_t} \right) \right\}$$

$$+ \frac{1}{S(S-\Omega_h)} \{....\} + \frac{1}{(S+\Omega_c)^2} \{....\} + \frac{1}{(S+\Omega_c)(S+2\Omega_c)} \{....\}$$

$$+ \frac{1}{(S-\Omega_h)(S-2\Omega_h)} \{....\} + \frac{1}{(S-\Omega_h)^2} \{....\} \Bigg]$$

$$+ e^{-S\bar{\tau}_{34}} [....]$$

$$+ e^{-S\bar{\tau}_{61}} [....]$$

$$= 0 . \tag{43}$$

Table II. Conditions for the Sample Calculation

L	5.5 m	α	~0.3
ℓ_o	4.0 m	ρ_f	1480 kg/m^3
D	0.05 m	ρ_g	10.65 kg/m^3
$\bar{\Lambda}_2 + \bar{\Lambda}_5 + \ell_o$	~9 m	Q	15.1 liter/min. (~4 gpm)

Furthermore it is assumed

$$S >> 1 , \tag{44}$$

which physically implies that the period of oscillations is relatively small. Then, only the polinomial terms in Eq. (43) may be retained, and with the terms containing the order smaller than S^{-1} may be neglected as a first order approximation. Thus

$$H(S) \doteq S\,\{\bar{\tau}_{34} + \bar{\tau}_{61}\} + \left\{K + \frac{f_\ell}{D}\,(\bar{\Lambda}_2 + \bar{\Lambda}_5 + \ell_o) + \frac{f_t}{D}\,(2L - \bar{\Lambda}_2 - \bar{\Lambda}_5)\right\}$$
$$+ \frac{1}{S}\left\{2\,\frac{g}{\bar{u}_\ell}\left(1 - \frac{\bar{u}_\ell}{\bar{u}_t}\right)\right\} = 0 \, . \tag{45}$$

Since from the continuity equation $\bar{\rho}_t\bar{u}_t = \bar{\rho}_\ell\bar{u}_\ell$, Eq. (38) for the manometer oscillation can be readily obtained from Eq. (45) using Eqs. (15) and (18).

In Fig. 3(d), the average volumetric flow rate is shown to be ~3 liter/min. (~0.8 gpm), and the average velocity becomes ~2.6 cm/sec. The residence time mainly depends on the length of the liquid region (~9 m) since the residence time in the two-phase region is shorter due to the increase of velocity. Thus the residence time of a fluid around the loop is approximately 350 sec., which is somewhat close to the ~3 min. period of oscillation in Fig.

3. It is well known that the period of the density (or enthalpy) wave oscillation is close to the residence time of a fluid around the loop [8], and the oscillation of ~3 min. period can be regarded as the density (or enthalpy) wave oscillation.

IV. Summary and Conclusions

The experiments on the two-phase natural circulation have been performed using the Freon-113 flow visualization loop. The two-phase flow was started as the unsteady, cyclic behavior involving sudden flashing and suppression of boiling with flow termination. This unsteady flow behavior is followed by a quasi-steady state, stabilized flow with certain regular patterns of flow oscillations having the ranges of periods in 8~35 seconds and 2.5~4 minutes. In order to find out the nature of these oscillations, one-dimensional field equations for the single-phase (liquid) and two-phase regions were set up, and the momentum equations were decoupled from the other equations to integrate along the loop. The homogeneous flow model was used for the two-phase region. Then the characteristic equation was derived using the perturbation method with the linearization assumption. The non-equilibrium effects and pressure effect on the density were not considered in present case. The characteristic equation derived can be used to find out the stability criteria (i.e., the onset of the instability) for the system. The simplified approach showed that the short-period oscillation is the manometer oscillation. It was shown that the same result could be obtained from the characteristic equation derived. The longer period oscillation turned out to be the density (or enthalpy) wave oscillation which has the period of oscillation close to the residence time of a fluid around the loop.

References

[1] Ishii, M., Lee, S.Y. and Abou El-Seoud, S., "Results of Two-phase Natural Circulation in Hot-leg U-bend Simulation Experiments," Proc. of the 15th Water Reactor Safety Information Meeting, NUREG/CP-0091, 1988.

[2] Ishii, M. and Kataoka, I., "Similarity Analysis and Scaling Criteria for LWR's under Single-phase and Two-phase Natural Circulation," NUREG/CR-3267, ANL-83-32, 1983.

[3] Ishii, M. and Kataoka, I., "Scaling Laws for Thermal-hydraulic System under Single-phase and Two-phase Natural Circulation," Nucl. Eng. & Design, Vol. 81, pp. 411-425, 1984.

[4] Kocamustafaogullari, G. and Ishii, M., "Scaling Criteria for Two-phase Flow Natural and Forced Convection Loop and Their Application to Conceptual 2x4 Simulation Loop Design," NUREG/CR-3420, ANL-83-61, 1983.

[5] Kocamustafaogullari, G. and Ishii, M., "Scaling Criteria for Two-phase Flow Loop and Their Application to Conceptual 2x4 Simulation Loop Design, Nucl. Tech., Vol. 65, pp. 146-160, 1984.

[6] Kocamustafaogullari, G. and Ishii, M., "Reduced Pressure and Fluid to Fluid Scaling Laws for Two-phase Flow Loop," NUREG/CR-4584, ANL-86-19, 1986.

[7] Lee, S.Y. and Ishii, M., "Simulation Experiments on Two-phase Natural Circulation in a Freon-113 Flow Visualization Loop," NUREG/CR-5082, ANL-88-1, 1988.

[8] Ishii, M., "Study on Flow Instabilities in Two-phase Mixtures," Argonne National Laboratory Report, ANL-76-23, 1976.

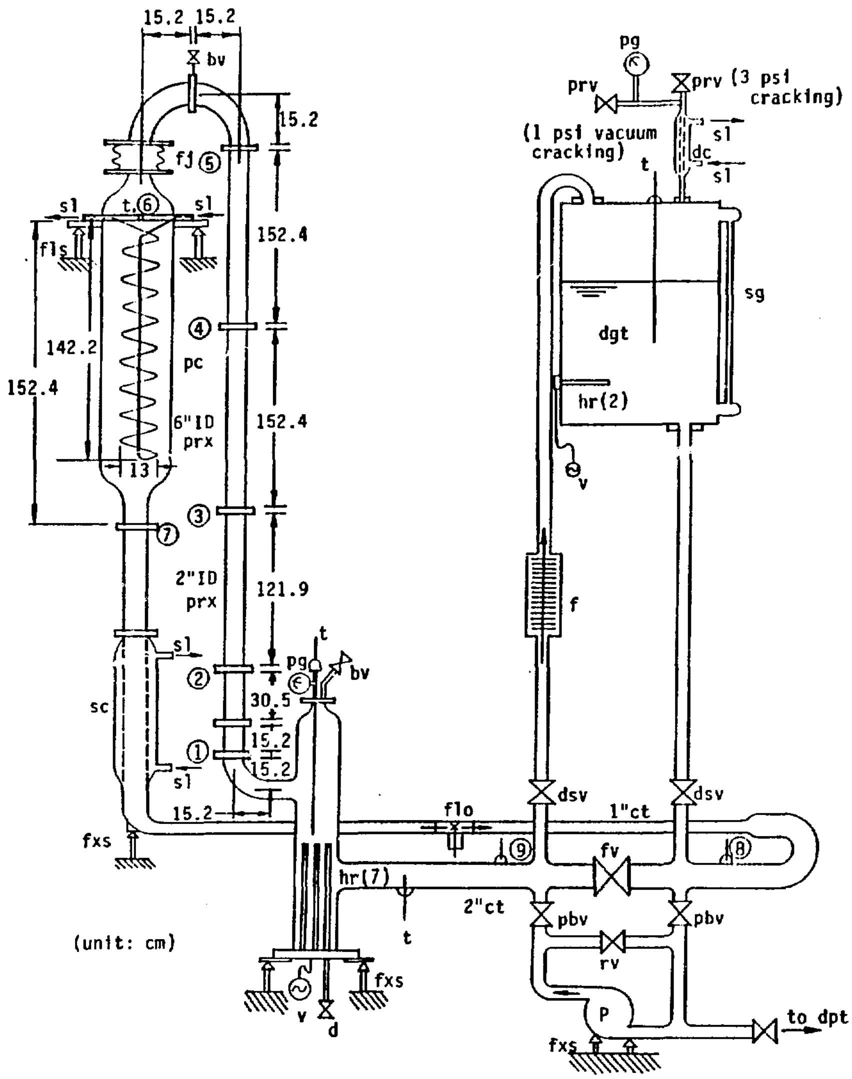

bv	bleed valve	P	pump (1.5 HP)
ct	copper tube (nominal size)	pbv	pump bypass valve
d	drain	pc	primary condenser (40 coil/ ¼" ct)
dc	dgt condenser (1" & 1¼" conc. ct)		
dgt	degassing tank	pg	pressure gauge
dpt	dump tank	prv	pressure relief valve
dsv	degassing tank shut-off valve	prx	pyrex test section
f	filter	rv	recirculate valve
fj	flexible joint	sc	subcooler (2" & 2½" conc. ct)
flo	flowmeter	sg	sight glass
fls	flexible support	sl	flow to/from secondary loop
fxs	fixed support	t	thermocouple
fv	friction control valve	v	variable transformer (0-4 KVA)
hr	heating rod (7x600 W, 2x750 W)	①-⑨	pressure tap

Fig. 1. Schematic of Freon-113 Flow Visualization Loop for Two-phase Natural Circulation Study

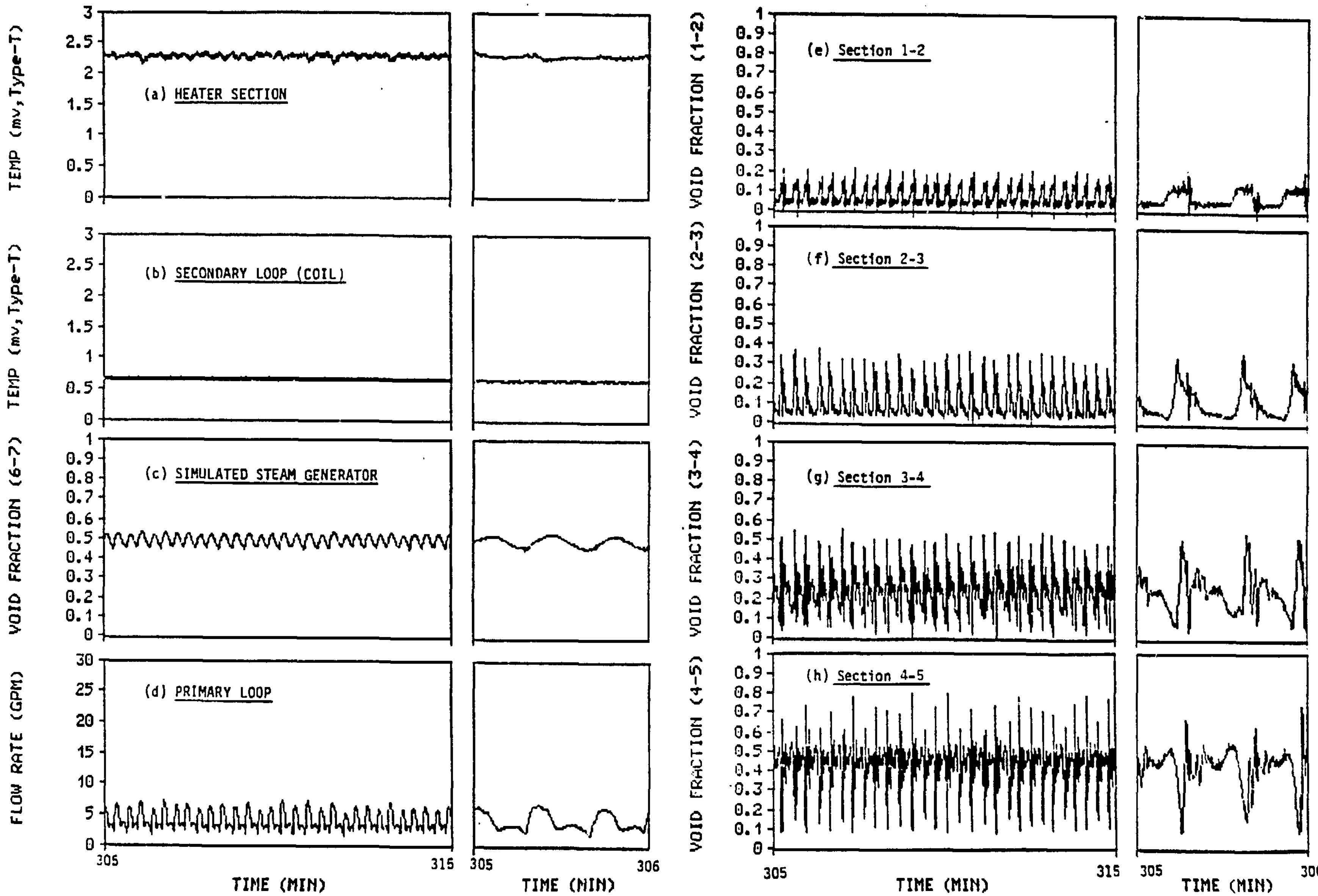

Fig. 2. Flow Behavior at Quasi-steady State (Type 1 Oscillation, Friction Control Valve Full-open, Power Input 2.2 KW, High Cooling)

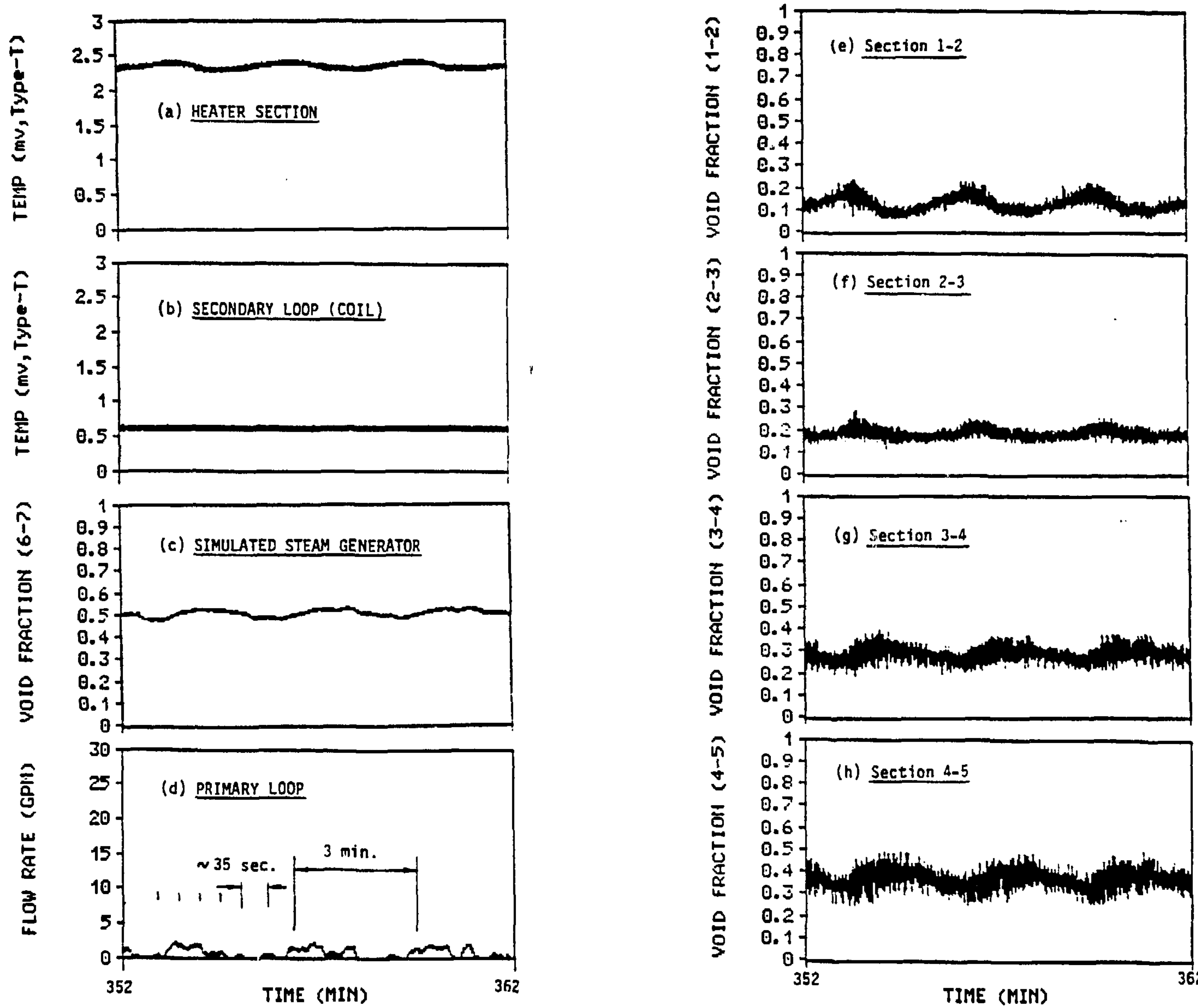

Fig. 3. Flow Behavior at Quasi-steady State (Type 2 Oscillation, Friction Control Valve 1/4-open, Power Input 2.2 KW, High Cooling)

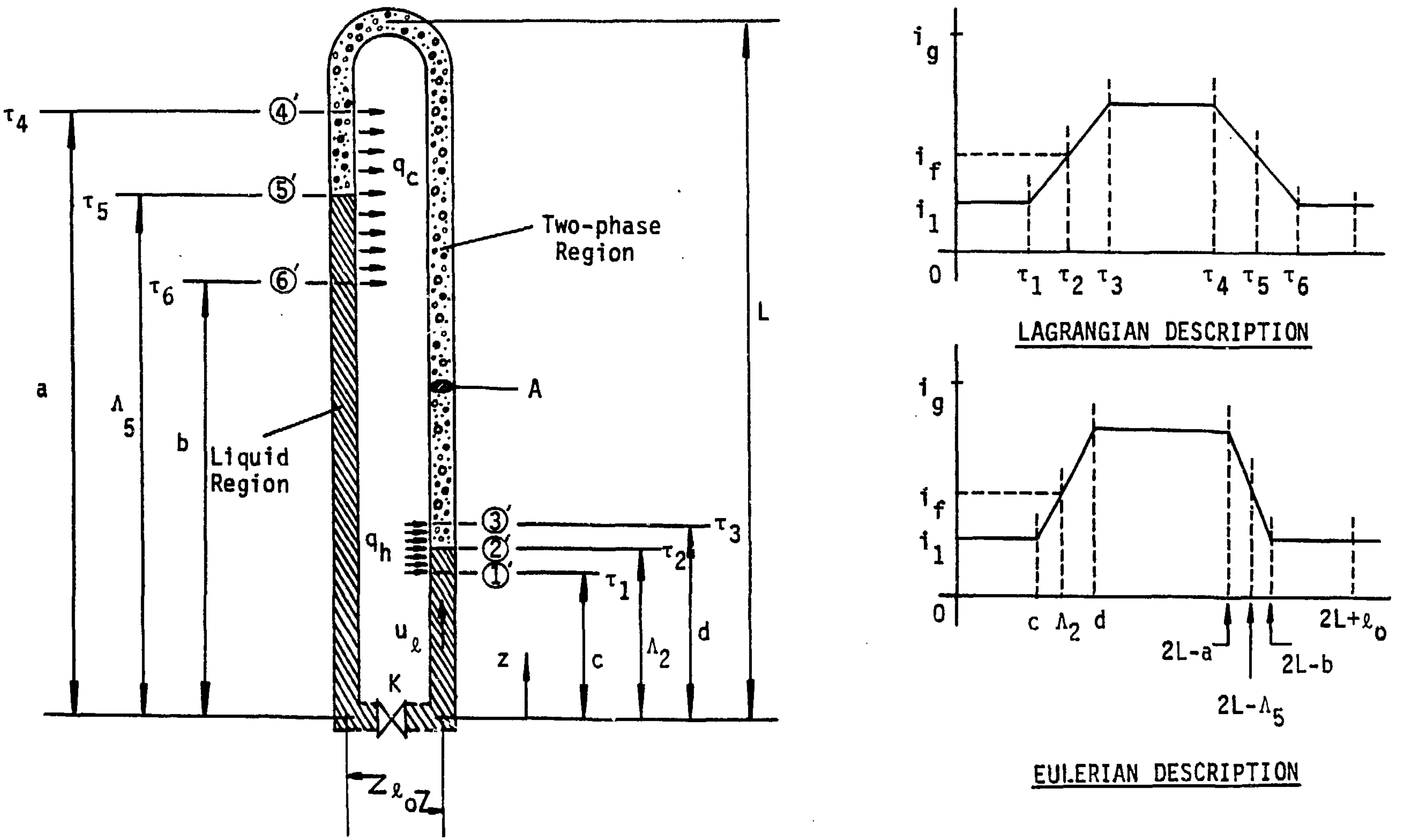

ℓ_o: HORIZONTAL SECTION OF THE LOOP

Fig. 4. Modelling of Flow Oscillation